Supporting Information for

Carborane Based Optoelectronically Active Organic Molecules: Wide Band-Gap Host Materials for Blue Phosphorescence

Kyung-Ryang Wee,[†] Yang-Jin Cho,[†] Soyeong Jeong,[†] Soonnam Kwon,[†,*] Jong-Dae Lee,[‡] Il-Hwan, Suh,[†] and Sang Ook Kang[†,*]

[†]Department of Advanced Material Chemistry, Korea University, Sejong, Chungnam 339-700, South Korea. [‡]Department of Chemistry, Chosun University, Gwangju, South Korea.

Contents

Scheme S1. Synthetic routes for **o-Bz**, **m-Bz**, and **p-Bz**. S3

Figure S1. ORTEP drawing of **p-Bz**. S3

Table S1. Crystal Data and Structure Refinement for **p-Bz** S4

Table S2. Selected Bond Lengths [Å] and Angles [^{o}] of **p-Bz** S5

Figure S2. Cyclic voltammograms of **o-Bz**, **m-Bz**, and **p-Bz**. S6

Table S3. Oxidation and Reduction Potentials of **o-Bz**, **m-Bz**, and **p-Bz** S6

Figure S3. Differential scanning calorimetry (DSC) sequent thermograms. S7

Figure S4. Double logarithmic representation of the TOF transients (hole). S8

Figure S5. Double logarithmic representation of the TOF transients (electron). S8

Table S4. Fitting Parameters of the Mobility of the Compounds to the Poole-Frenkel Function S9

Synthetic routs for three compounds, **o-**, **m-**, and **p-Bz**, are shown in Scheme S1. For comparison with **p-Cb**, of which detailed crystal structures can be found in Ref. 1, crystal structure data for **p-Bz** are shown in Figure S1 and Table S1. Cyclic voltametric data for **o-**, **m-**, and **p-Bz** are presented in Figure S2 and Table S2. For determination of the thermal properties, such as glass transition temperature and melting point, differential scanning calorimetry (DSC) data are shown in Figure S3. The raw data used for obtaining charge mobility are presented in Figure S4 and S5. In Table S3, fitting parameters of charge mobility as a function of the electric field to the Poole-Frenkel function[2] for each compound are shown. Also, the complete citation of Ref. 13 in manuscript is listed in Ref. 3.

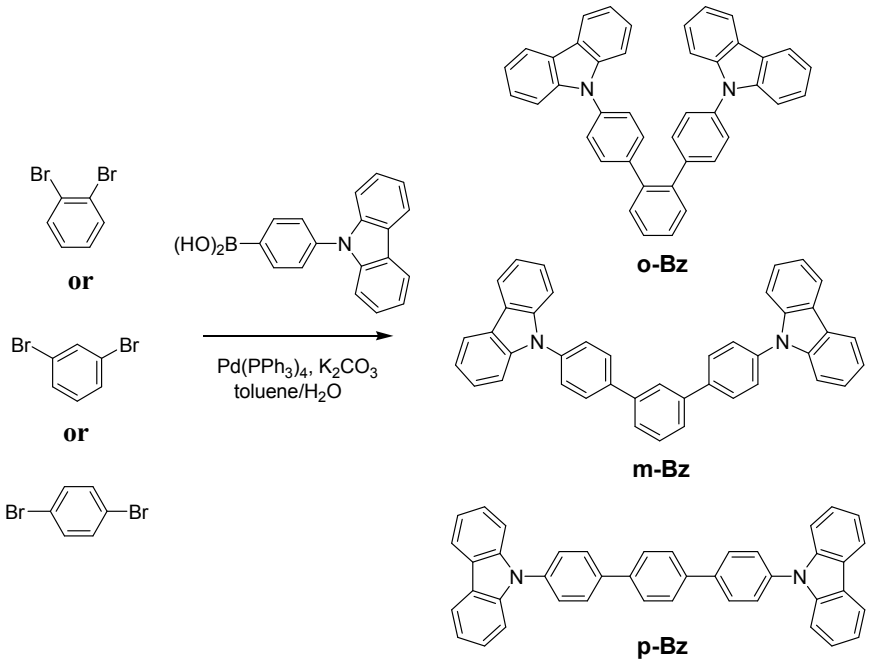

Scheme S1. Synthetic routes for **o-Bz, m-Bz**, and **p-Bz**.

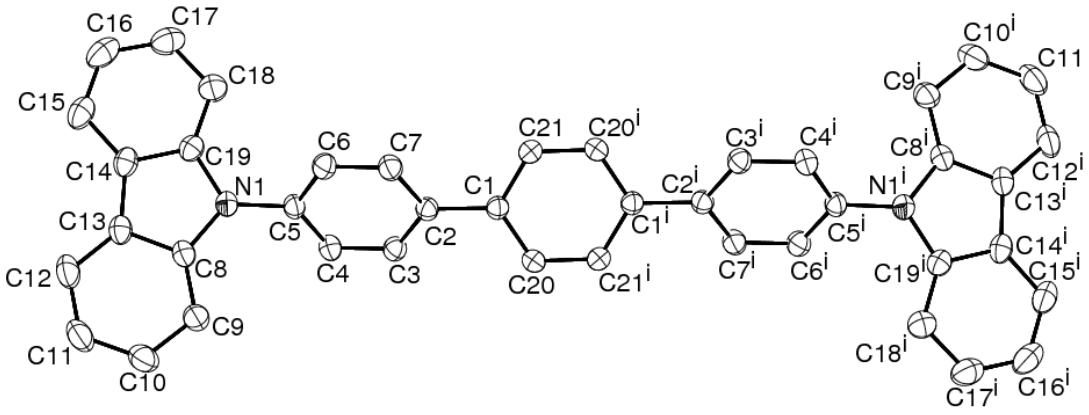

Figure S1. ORTEP drawing (30% probability for thermal ellipsoids) of **p-Bz**. The hydrogen atoms are omitted for clarity.

Table S1. Crystal Data and Structure Refinement for **p-Bz**[a,b]

	p-Bz
Empirical formula	$C_{42}\ H_{28}\ N_2$
Formula weight	560.66
Crystal system, space group	Monoclinic, P1 21/n 1
Unit cell dimensions	a = 5.4579(15) Å α = 90.0°
	b = 12.568(4) Å β = 93.467°
	c = 21.459(6) Å γ = 90.0°
Volume	1469.3(7) Å^3
Z, Calculated density	2, 1.267 mg/m^3
μ	0.073 mm^{-1}
F(000)	588
Crystal size	0.32 x 0.28 x 0.42 mm
θ range for data collection	1.88 to 28.38°
Limiting indices	$-7 \le h \le 7$, $-16 \le k \le 16$,
	$-25 \le l \le 28$
Reflections collected / unique	9706 / 3610 [R_{int} = 0.0305]
Max. and min. transmission	0.9903 and 0.9808
Completeness to theta = 28.43	97.9%
Refinement method	Full-matrix least-squares on F^2
Data / restraints / parameters	3610 / 0 / 200
Goodness-of-fit on F^2	1.030
Final R indices [$I>2\sigma(I)$]	R_1 = 0.0446, wR_2 = 0.1009
R indices (all data)	R_1 = 0.0971, wR_2 = 0.1288
Largest diff. peak and hole	0.188 and -0.174 e. Å^{-3}

[a] $R_1 = \sum||F_o|-|F_c||$ (based on reflections with $F_o^2>2\sigma F^2$) [b] $wR_2 = [\sum[w(F_o^2-F_c^2)^2]/\sum[w(F_o^2)^2]]^{1/2}$; $w = 1/[\sigma^2(F_o^2)+(0.095P)^2]$; $P = [\max(F_o^2, 0)+2F_c^2]/3$(also with $F_o^2>2\sigma F^2$)

Table S2. Selected Bond Lengths [Å] and Angles [°] of **p-Bz**

Bond lengths [Å]		Bond Angles [°]	
C(1)-C(20)	1.386(2)	C(20)-C(1)-C(21)	116.98(14)
C(1)-C(21)	1.393(2)	C(20)-C(1)-C(2)	122.20(15)
C(1)-C(2)	1.481(2)	C(21)-C(1)-C(2)	120.81(14)
C(2)-C(7)	1.391(2)	C(7)-C(2)-C(3)	117.20(15)
C(2)-C(3)	1.393(2)	C(7)-C(2)-C(1)	120.76(15)
C(3)-C(4)	1.381(2)	C(3)-C(2)-C(1)	122.03(15)
C(4)-C(5)	1.376(2)	C(4)-C(3)-C(2)	121.50(16)
C(5)-C(6)	1.386(2)	C(5)-C(4)-C(3)	120.16(16)
C(5)-N(1)	1.4252(19)	C(4)-C(5)-C(6)	119.27(15)
C(6)-C(7)	1.373(2)	C(4)-C(5)-N(1)	121.18(15)
C(8)-C(9)	1.384(3)	C(6)-C(5)-N(1)	119.54(15)
C(8)-N(1)	1.393(2)	C(7)-C(6)-C(5)	120.28(16)
C(8)-C(13)	1.404(2)	C(6)-C(7)-C(2)	121.55(16)
C(9)-C(10)	1.383(2)	C(9)-C(8)-N(1)	129.42(16)
C(10)-C(11)	1.382(3)	C(9)-C(8)-C(13)	121.48(16)
C(11)-C(12)	1.374(3)	N(1)-C(8)-C(13)	109.01(15)
C(12)-C(13)	1.391(3)	C(10)-C(9)-C(8)	117.75(18)
C(13)-C(14)	1.444(3)	C(9)-C(10)-C(11)	121.4(2)
C(14)-C(15)	1.389(3)	C(12)-C(11)-C(10)	120.94(19)
C(14)-C(19)	1.402(2)	C(11)-C(12)-C(13)	119.08(19)
C(15)-C(16)	1.372(3)	C(12)-C(13)-C(8)	119.35(18)
C(16)-C(17)	1.386(3)	C(12)-C(13)-C(14)	133.75(18)
C(17)-C(18)	1.376(3)	C(8)-C(13)-C(14)	106.81(15)
C(18)-C(19)	1.384(3)	C(15)-C(14)-C(19)	119.11(19)
C(19)-N(1)	1.394(2)	C(15)-C(14)-C(13)	133.94(18)
C(20)-C(21)	1.381(2)	C(19)-C(14)-C(13)	106.94(15)
C(21)-C(20)	1.381(2)	C(16)-C(15)-C(14)	119.3(2)
		C(15)-C(16)-C(17)	120.8(2)
		C(18)-C(17)-C(16)	121.5(2)
		C(17)-C(18)-C(19)	117.6(2)
		C(18)-C(19)-N(1)	129.25(16)
		C(18)-C(19)-C(14)	121.72(17)
		N(1)-C(19)-C(14)	109.00(15)
		C(21)#1-C(20)-C(1)	121.30(16)
		C(20)#1-C(21)-C(1)	121.72(15)
		C(8)-N(1)-C(19)	108.23(14)
		C(8)-N(1)-C(5)	125.52(14)
		C(19)-N(1)-C(5)	124.82(14)

Electrochemical Properties

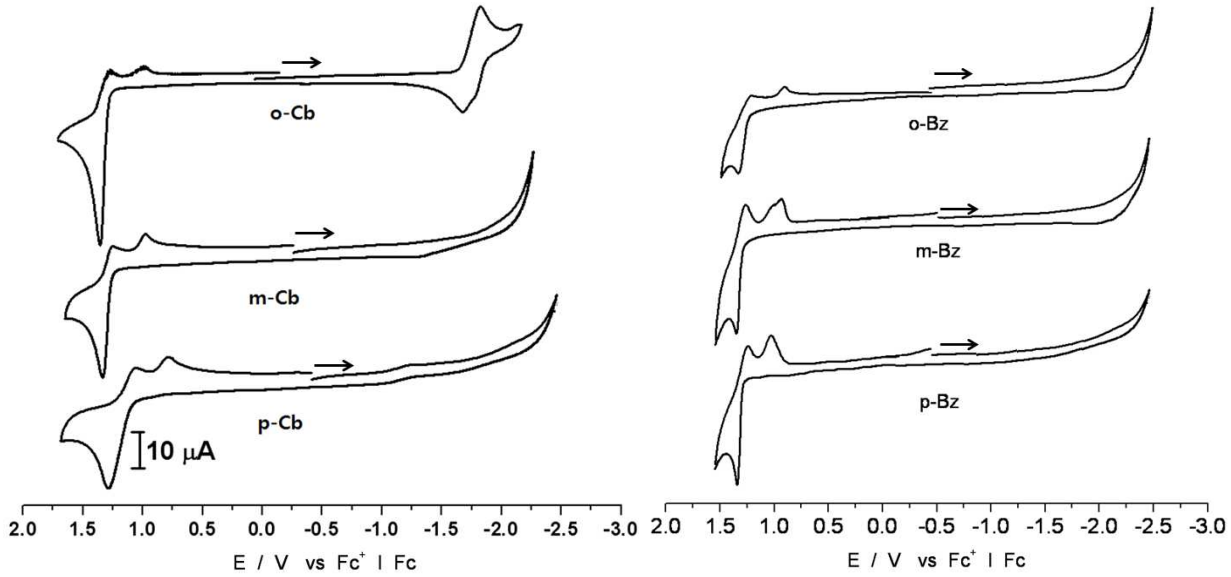

Figure S2. Cyclic voltammograms of **o-Cb**, **m-Cb**, **p-Cb**, **o-Bz**, **m-Bz**, and **p-Bz** for 0.1 mM CH_2Cl_2 solution containing 0.1 M TBAP taken at a scan rate of 0.1V s^{-1} and all scans go in the negative direction.

Table S3. Oxidation and Reduction Potentials [a]

Entry	Oxidation (V vs Fc^+/Fc)					Reduction (V vs Fc^+/Fc)				
	E_{pa1}	E_{pa2}	E_{pc1}	E_{pc2}	E_{onset}^{ox}	E_{pa1}	E_{pa2}	E_{pc1}	E_{pc2}	$E_{1/2}^{red}$
o-Cb	1.26	-[b]	1.18	0.96	1.22	-1.75	-1.81	-2.01	-[b]	-1.88
m-Cb	1.26	-[b]	1.20	0.93	1.25	-[b]	-[b]	-[b]	-[b]	-[b]
p-Cb	1.39	-[b]	1.18	0.92	1.24	-[b]	-[b]	-[b]	-[b]	-[b]
o-Bz	1.31	-[b]	1.28	0.98	1.24	-[b]	-[b]	-[b]	-[b]	-[b]
m-Bz	1.31	-[b]	1.22	0.98	1.24	-[b]	-[b]	-[b]	-[b]	-[b]
p-Bz	1.31	-[b]	1.22	1.04	1.25	-[b]	-[b]	-[b]	-[b]	-[b]

[a]CVs were recorded at room temperature in Ar purged CH_2Cl_2/0.1 M TBAP. [b]Not observed.

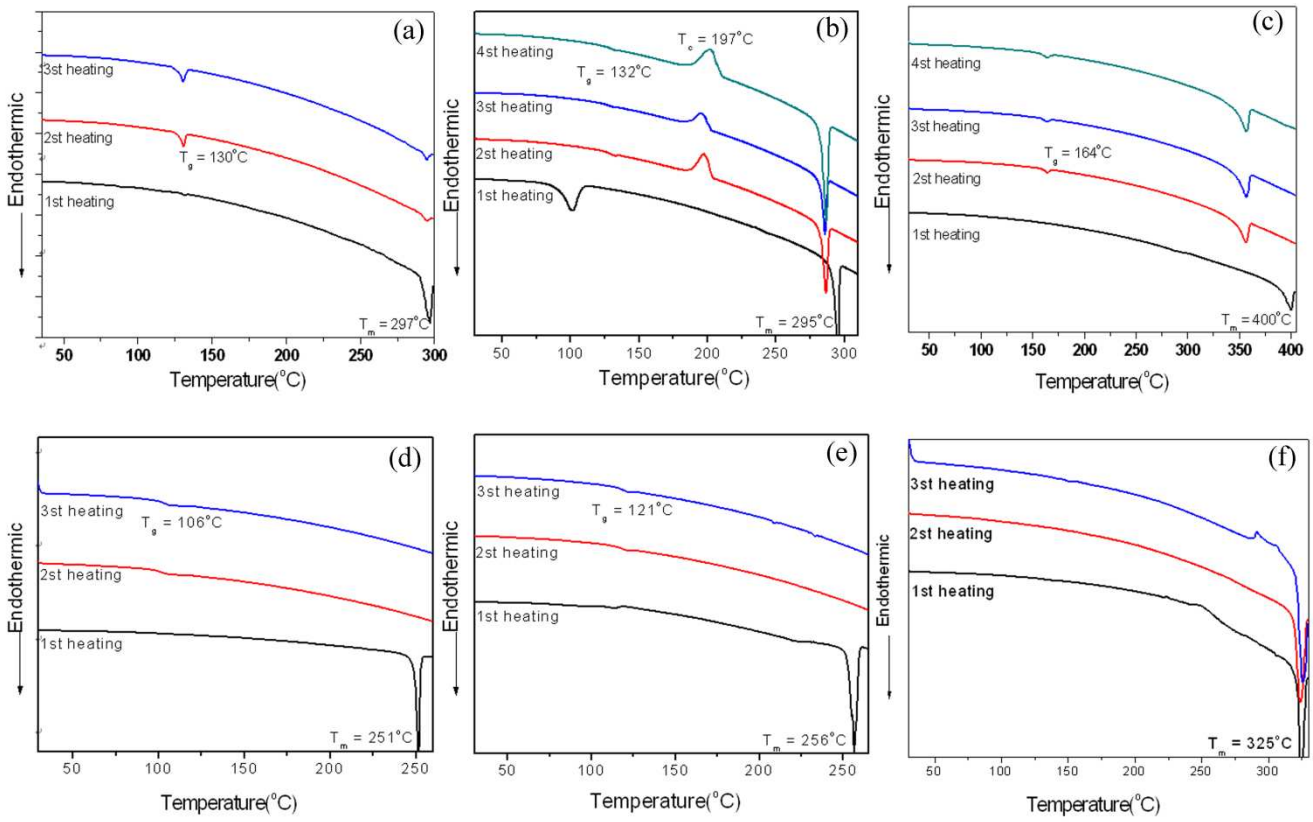

Figure S3. Differential scanning calorimetry (DSC) sequent thermograms for (a) **o-Cb**, (b) **m-Cb**, (c) **p-Cb**, (d) **o-Bz**, (e) **m-Bz**, and (f) **p-Bz** with sequential heating and cooling.

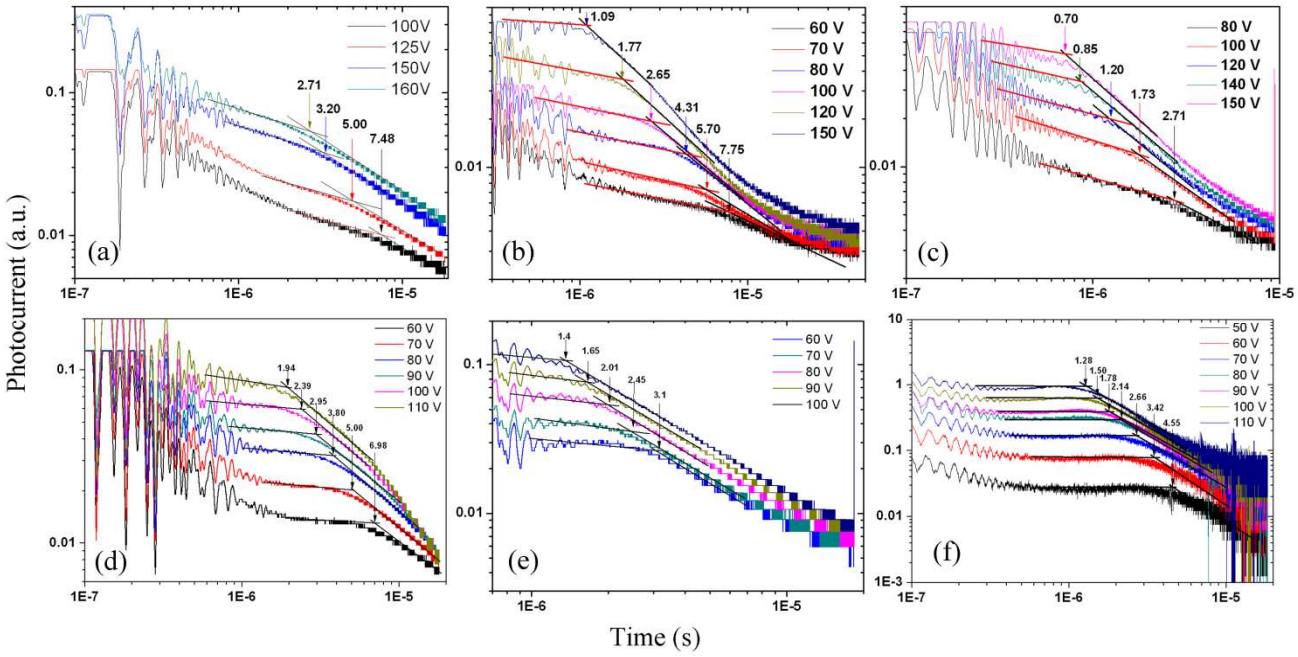

Figure S4. Double logarithmic representation of the TOF transients (hole) for (a) **o-Cb**, (b) **m-Cb**, (c) **p-Cb**, (d) **o-Bz**, (e) **m-Bz**, and (f) **p-Bz** under various voltages.

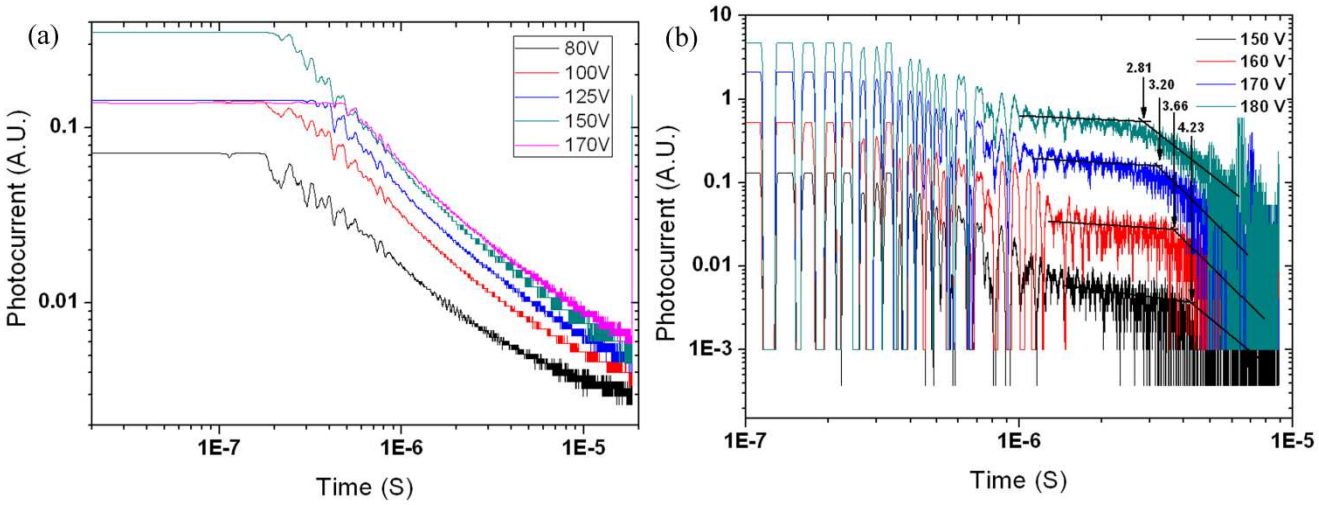

Figure S5. Double logarithmic representation of the TOF transients (electron) for (a) **p-Cb** and (b) **p-Bz** under various voltages.

Table S4. Fitting Parameters for the Mobility of the Compounds to the Poole-Frenkel Function ($\mu=\mu_o$ $\exp(E^{1/2}/\sigma)$).

	μ_0		σ		Statistics	
	Value	Error	Value	Error	Reduced Chi-Sqr	Adj. R-Square
o-Cb	1.41E-5	2.99E-6	263.16	22.08	3.02E-11	0.98243
m-Cb	3.75E-5	2.34E-6	243.90	6.18	6.53E-11	0.99707
p-Cb	7.28E-5	1.11E-5	256.41	16.26	5.50E-10	0.98668
o-Bz	6.73E-05	6.30E-06	303.03	15.82	6.65E-11	0.98700
m-Bz	1.82E-04	4.60E-06	454.55	10.03	7.53E-12	0.99811
p-Bz(hole)	2.17E-04	6.11E-06	384.62	8.47	4.29E-11	0.99729
p-Bz(el)	1.85E-05	4.08E-6	270.27	2.34	1.16E-13	0.99977

References

1. Wee, K.-R.; Han, W.-S.; Cho, D. W.; Kwon, S.; Pac, C.; Kang, S. O. *Angew. Chem. Int. Ed.* **2012**, *51*, 2677.

2. Gill, W. D., *J. Appl. Phys.* **1972**, 43, 5033

3. Frisch, M. J.; Trucks, G. W.; Schlegel, H. B.; Scuseria, G. E.; Robb, M. A.; Cheeseman, J. R.; Scalmani, G.; Barone, V.; Mennucci, B.; Petersson, G. A.; Nakatsuji, H.; Caricato, M.; Li, X.; Hratchian, H. P.; Izmaylov, A. F.; Bloino, J.; Zheng, G.; Sonnenberg, J. L.; Hada, M.; Ehara, M.; Toyota, K.; Fukuda, R.; Hasegawa, J.; Ishida, M.; Nakajima, T.; Honda, Y.; Kitao, O.; Nakai, H.; Vreven, T.; Montgomery Jr., J. A.; Peralta, J. E.; Ogliaro, F.; Bearpark, M.; Heyd, J. J.; Brothers, E.; Kudin, K. N.; Staroverov, V. N.; Keith, T.; Kobayashi, R.; Normand, J.; Raghavachari, K.; Rendell, A.; Burant, J. C.; Iyengar, S. S.; Tomasi, J.; Cossi, M.; Rega, N.; Millam, J. M.; Klene, M.; Knox, J. E.; Cross, J. B.; Bakken, V.; Adamo, C.; Jaramillo, J.; Gomperts, R.; Stratmann, R. E.; Yazyev, O.; Austin, A. J.; Cammi, R.; Pomelli, C.; Ochterski, J. W.; Martin, R. L.; Morokuma, K.; Zakrzewski, V. G.; Voth, G. A.; Salvador, P.; Dannenberg, J. J.; Dapprich, S.; Daniels, A. D.; Farkas, O.; Foresman, J. B.; Ortiz, J. V.; Cioslowski, J.; Fox, D. J., Gaussian 09, Revision B.01, Gaussian, Inc., Wallingford CT, 2010.